Electronic Supplementary Material (ESI) for Energy & Environmental Science.
This journal is © The Royal Society of Chemistry 2020

Supporting Information

Universal Approach toward High-efficiency Two-dimensional Perovskite Solar Cells via Vertical-Rotation Process

Yi Yang,[1,2†] Cheng Liu,[1,2†] Arup Mahata,[3,4] Mo Li,[2,5] Cristina Roldán-Carmona,[2] Yong Ding,[1,2] Zulqarnain Arain,[1] Weidong Xu,[1] Yunhao Yang,[1] Pascal Alexander Schouwink,[2] Andreas Züttel,[2,5] Filippo De Angelis,[3,4,6,7] Songyuan Dai[1*] and Mohammad Khaja Nazeeruddin.[2*]*

[1]Beijing Key Laboratory of Novel Thin-Film Solar Cells, Beijing Key Laboratory of Energy Safety and Clean Utilization, North China Electric Power University, Beijing 102206, P. R. China.

[2]Institute of Chemical Sciences and Engineering, EPFL Valais, 1951, Sion, Switzerland.

[3]CompuNet, Istituto Italiano di Tecnologia, Via Morego 30, 16163 Genova, Italy.

[4]Computational Laboratory for Hybrid/Organic Photovoltaics (CLHYO) Istituto CNR di Scienze e Tecnologie Chimiche "Giulio Natta" (CNR-SCITEC) Via Elce di Sotto 8, 06123 Perugia, Italy.

[5]Empa Materials Science and Technology, CH-8600 Dübendorf, Switzerland.

[6]Department of Chemistry, Biology and Biotechnology, University of Perugia, Via Elce di Sotto 8, 06123 Perugia, Italy.

[7]Chemistry Department, College of Science, King Saud University, Riyadh, Saudi Arabia.

†These authors contributed equally to this work.

*Corresponding Author

E-mail: dingy@ncepu.edu.cn, sydai@ncepu.edu.cn and mdkhaja.nazeeruddin@epfl.ch

Computational details

First-principles calculations based on density functional theory (DFT) are carried out as implemented in the PWSCF Quantum-Espresso package.[1] Geometry optimization, including dispersion correction[2], is performed using GGA-PBE[3] level of theory and the electrons-ions interactions are described by ultrasoft pseudo-potentials[4] with electrons from I 5s, 5p; N, C 2s, 2p; H 1s; Pb, 6s, 6p, 5d; shells explicitly included in calculations. Plane wave basis set cutoffs for the smooth part of the wave functions and the augmented density were 40 and 320 Ry, respectively. The slabs are modeled by cutting the experimental $(PEA)_2(MA)_3Pb_4I_{13}$ crystal with the exposed (202) and (111) surface. Geometry optimizations are done with a 1 × 1 × 2 kpoint sampling for both (202) and (111) surfaces using the experimental cell parameters along the periodic direction of the slabs, whereas a vacuum of more than 10 Å is introduced along the surface truncation direction. Symmetric termination in the vacuum direction of the slabs are maintained by considering five Pb-I layers for 202 PbI_2-termination, whereas three Pb-I layers are maintained for 202 MAI-termination and 111-surface. Cationic molecules (NH_4^+, MA^+ and PEA^+) are optimized in 20×20×20 $Å^3$ isolated box with Gamma kpoint sampling. Adsorption energy is calculated using the following formula:

Adsorption energy = $E_{slab+cationic\ molecule\ adsorbed} - E_{slab} - E_{cationic\ molecule}$

where $E_{slab+cationic\ molecule\ adsorbed}$ represents the total energy of the adsorbed cationic molecules with the slab, E_{slab} is the total energy of the bare slab, and $E_{cationic\ molecule}$ is the energy of the isolated cationic molecule in a large supercell. The absolute values of the adsorption energies are large because of the adsorption of a gas-phase cationic molecule.

Experimental Section

Materials and Device Fabrication: The PbI_2 (>98.0%), PEAI (>98.0%), BAI (>97.0%), BDAI (>98.0%), PDAI (>98.0%) were purchased from the Tokyo Chemical Industry Co., LTD, and the NMAI (>99.0%) and MAI (>99.5%) were purchased from the Xi'an Polymer Light Technology Corp. All reagents were used as received without further purification. The PEDOT/PSS (Xi'an Polymer Light Technology Corp. CLEVIOS™ P VP AI 4083) was spin-coated on the cleaned FTO substrate at 5000 rpm for 45s and annealed at 120 ℃ for 30 min. The perovskite film deposition was carried out in a dry air glovebox. The ambient humidity was controlled by changing the airflow rate and was monitored by a precise hygrometer. The perovskite precursor solution (1M in DMF, with molar ratio of organic spacing cation: MAI: PbI_2 = 2: 3: 4) was spin-coated on the top of PEDOT/PSS at 5000 rpm for 30 s and annealed at 100℃ for 15 min. For the VR method, corresponding amounts of additives were added into the precursor, and all the other steps are same as those of the reference device. The electron transport layer of $PC_{61}BM$ (Xi'an Polymer Light Technology Corp., 20 mg mL^{-1} in chlorobenzene) and the hole-blocking layer of BCP (Xi'an Polymer Light Technology Corp., 0.5 mg mL^{-1} in isopropanol) were deposited at 3000 rpm for 30 s in sequence. Finally, a 70-nm-thick Ag electrode was thermally evaporated under high vacuum of $\sim 4 \times 10^{-6}$ Torr.

Device and Film Characterization: The PCE and current density-voltage (*J-V*) characteristics were measured using the sunlight simulator (XES-300T1, SAN-EI Electric) under simulated AM 1.5 G irradiation, which was calibrated using a standard silicon reference cell from Newport. The scanning rate is 50 mV s^{-1}. Devices were first measured in the forward scan from -0.2 V to 1.3 V, and then reverse scan from 1.3 V to -0.2 V. The scan step is 15 mV. The SEM images were taken with the SU8010 scanning electron microscope (Hitachi). XRD data were acquired using the Bruker X-ray diffractometer with a Cu Kα radiation source. Absorption spectra were measured with a UV-2450 spectrophotometer (Shimadzu). GIWAXS measurements were performed at the 1W1A beamline at the Beijing Synchrotron. 8.05 keV photons and

exposure times of 20 s were used. For XPS depth profiling, the samples were sputtered using an Ar^+ ion (2 keV) gun for 500 s before each measurement, and XPS analysis was performed using a Phoibos 150 (SPECS) energy analyzer with Mg Kα X-ray source (hν = 1253.6 eV). The binding energy was referenced to Sn $3d_{5/2}$ peak of FTO glass at 486.9 eV for charge compensation. The detailed measuring parameters and equipment for IPCE, TRPL, PL mapping, EIS, light intensity dependence and TPV measurements were described in our previous research.[5]

Figures and tables

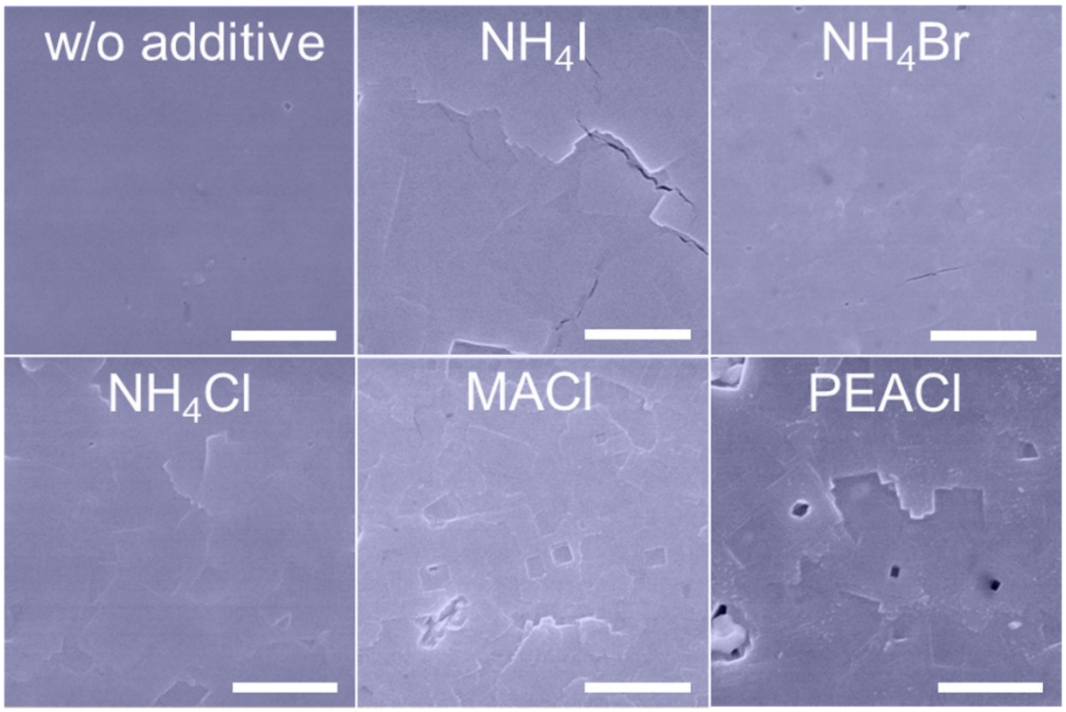

Fig. S1 Surface SEM images of the 2D $(PEA)_2(MA)_3Pb_4I_{13}$ films without/with additives. Scale bars, 500 nm.

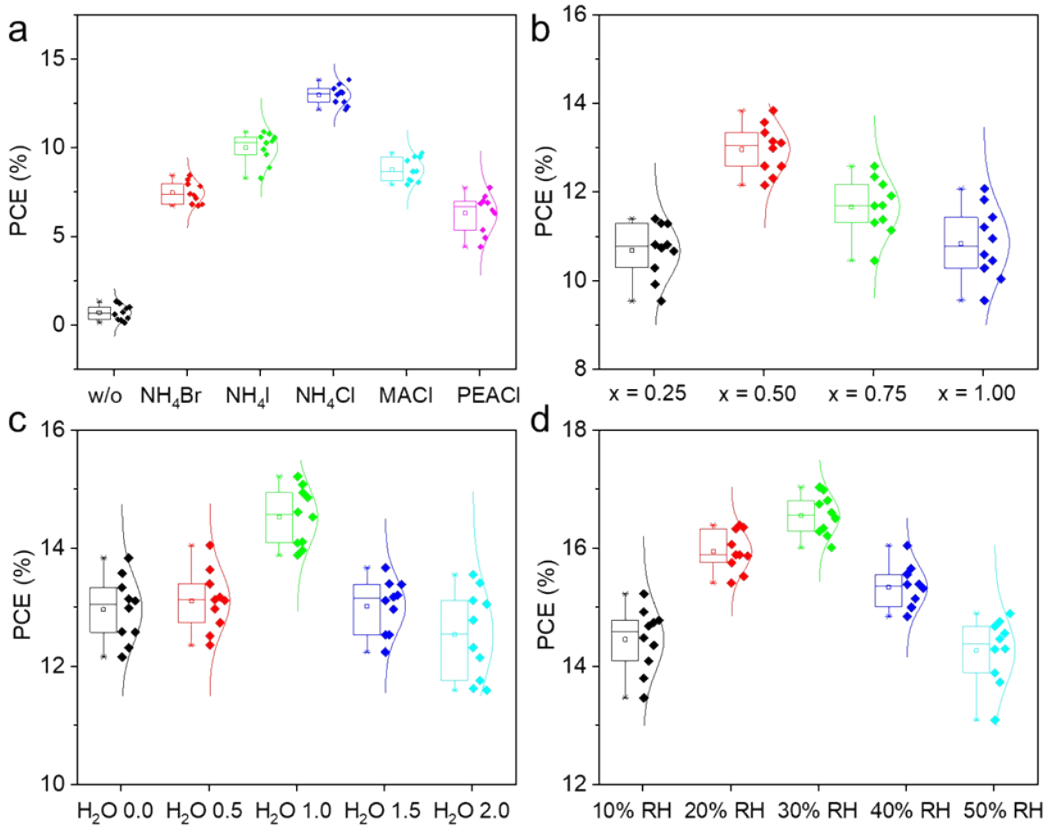

Fig. S2 Statistical distributions of PCEs for the different groups of perovskite solar cells. Devices fabricated (a) with different additives, (b) with different amounts of NH_4Cl addition (molar ratio of PEAI: MAI: PbI_2: NH_4Cl = 2: 3: 4: x), (c) with different amounts of H_2O addition (vol %) and (d) under different relative humidity (RH) values.

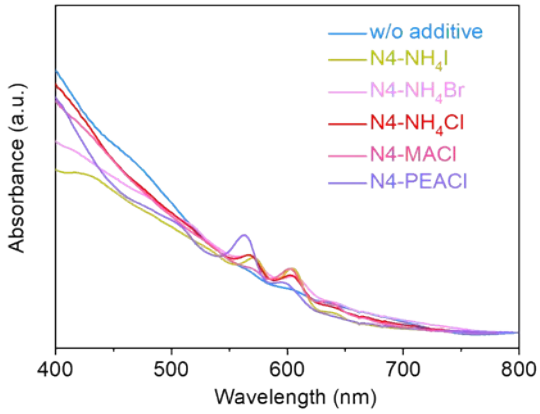

Fig. S3 Ultraviolet visible (UV-vis) spectra of different 2D perovskite films.

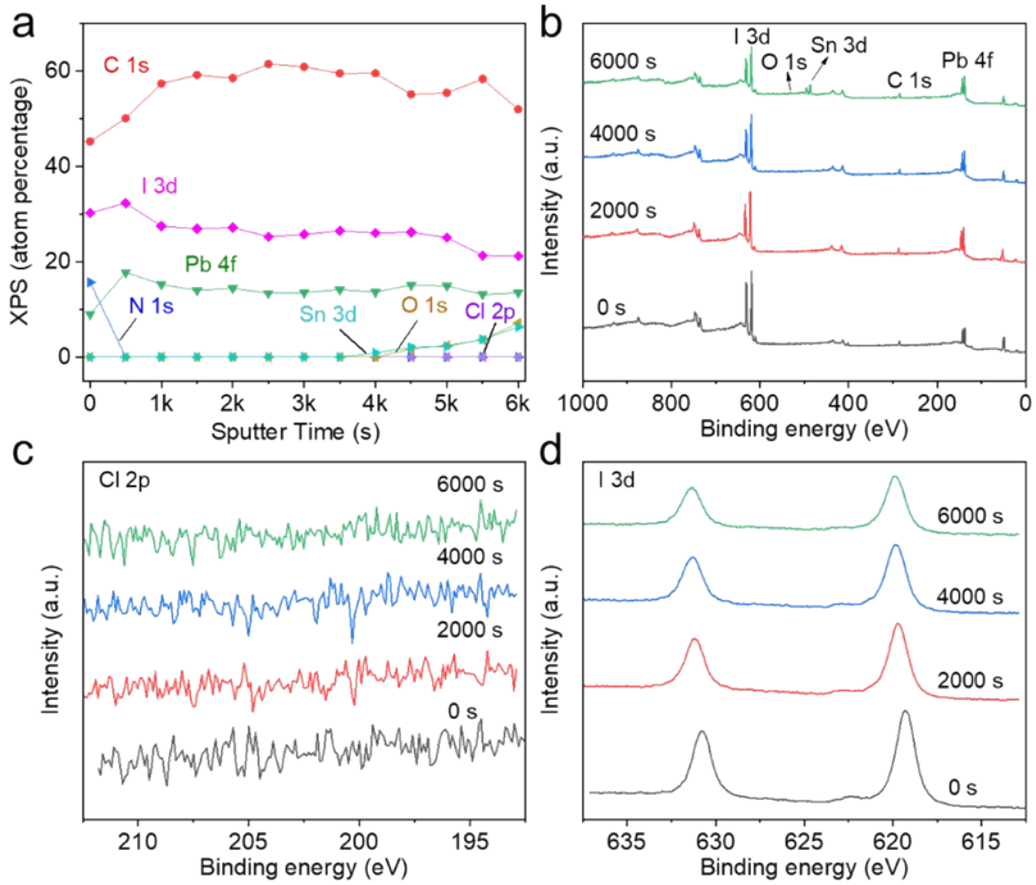

Fig. S4 (a) XPS depth profile analysis for the VR-2D perovskite film on FTO/PEDOT:PSS substrate. (b-d) XPS full spectra (b), Cl 2p high-resolution XPS spectra (c) and I 3d high-resolution XPS spectra (d) with different sputtering time.

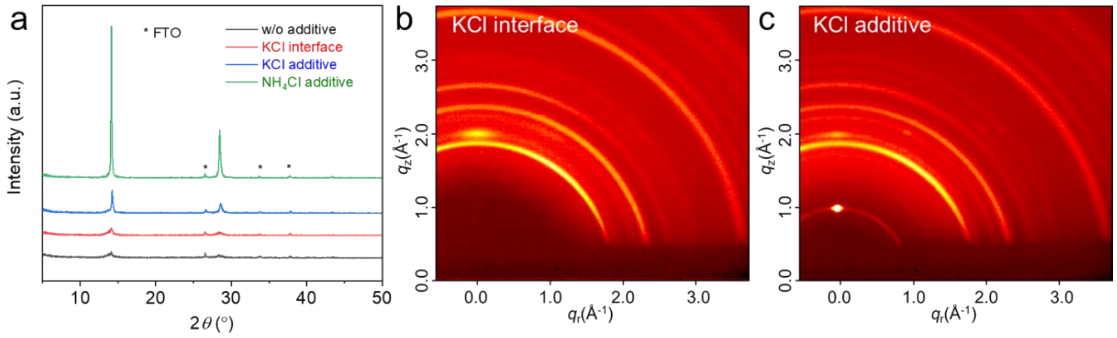

Fig. S5 (a) Normal XRD spectra for 2D perovskite films under different conditions. (b, c) 2D XRD images for 2D perovskite films prepared with KCl interface modification (b) and KCl additive (c).

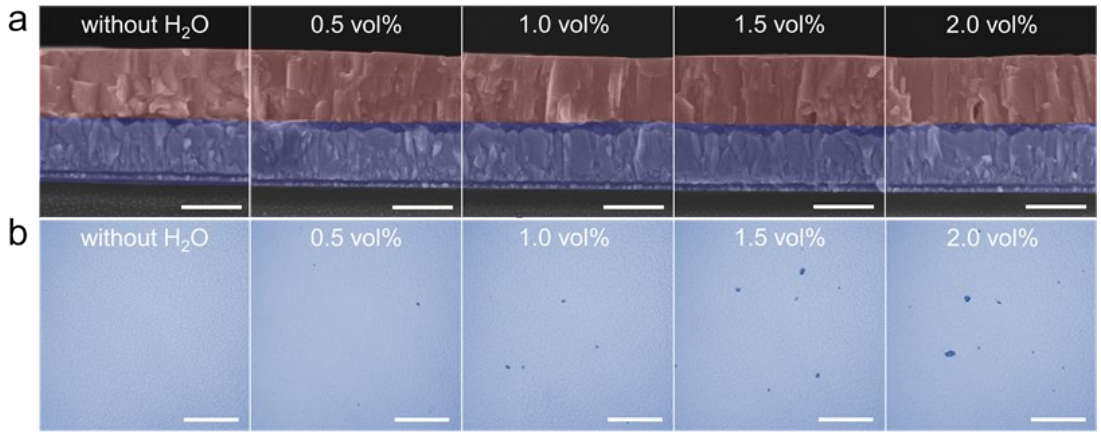

Fig. S6 (a) Cross-sectional SEM images and (b) metallographic microscope images of VR-2D films fabricated with different amounts of H_2O addition. Scale bars, 400 nm and 100 μm, respectively.

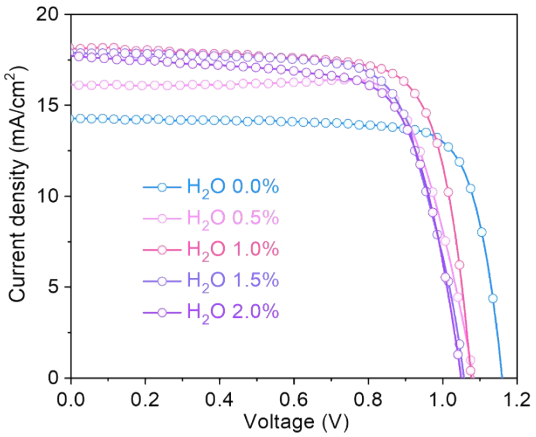

Fig. S7 *J-V* characteristics of VR-2D PSCs fabricated with different amounts of H_2O addition.

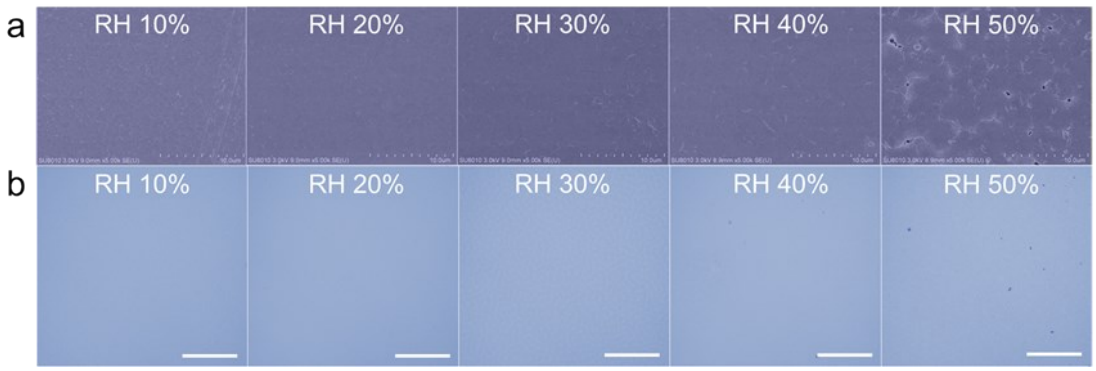

Fig. S8 (a) Surface SEM images and (b) metallographic microscope images of VR-2D films fabricated under various relative humidities from 10% to 50%. Scale bars, 100 μm, respectively.

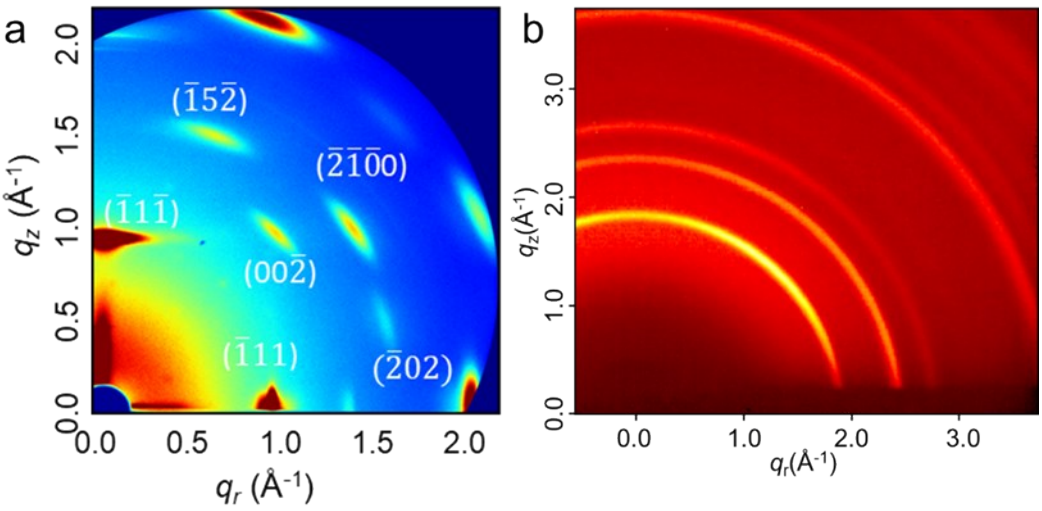

Fig. S9 (a) GIWAXS image of the VR-2D perovskite film prepared under 30% RH. (b) GIXRD image of the FTO substrate.

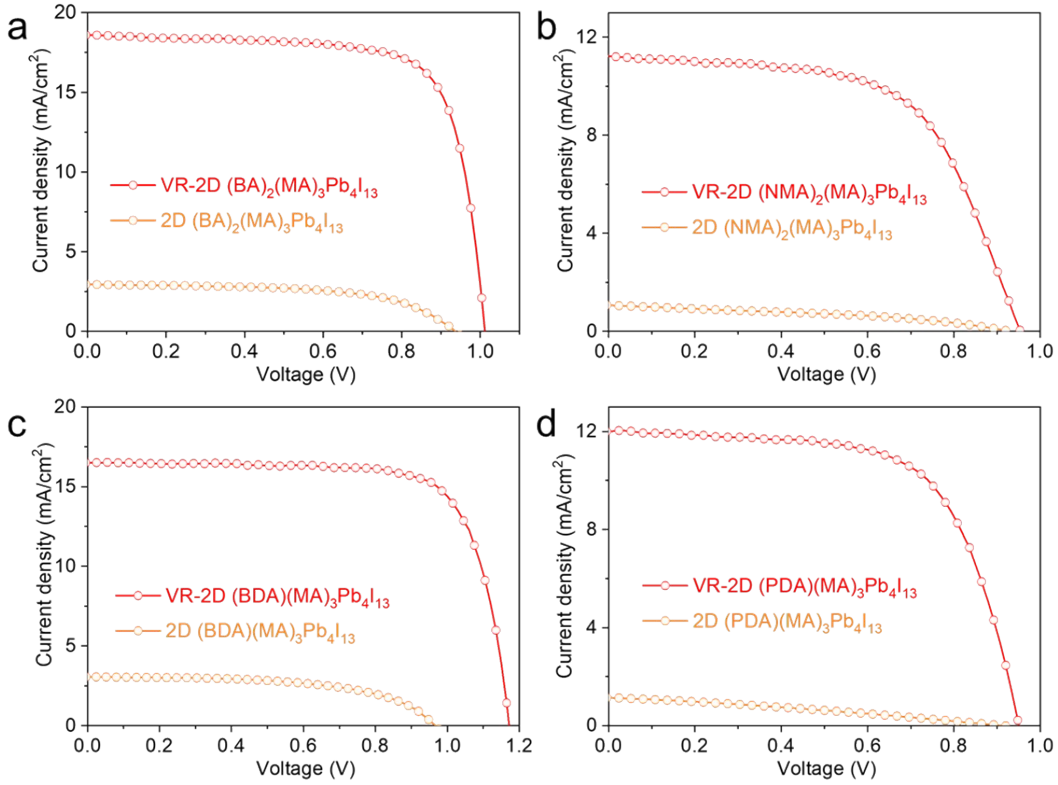

Fig. S10 *J-V* curves of the five typical 2D PSCs using the VR method.

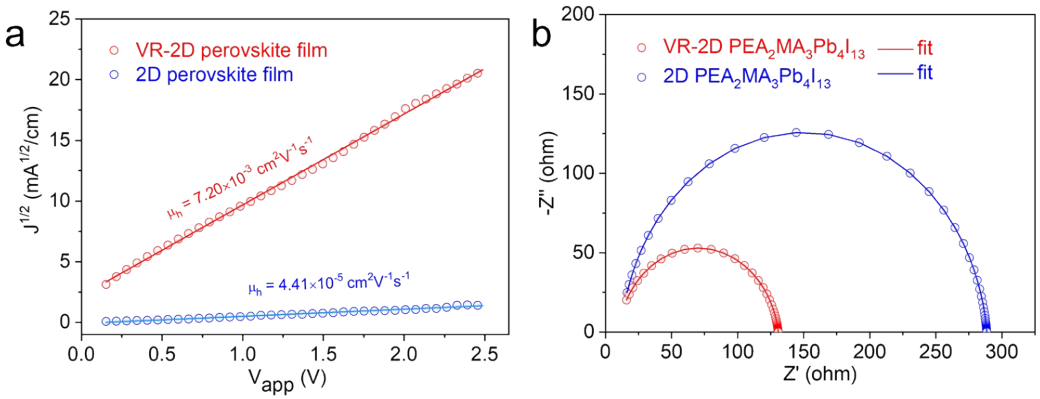

Fig. S11 (a) Dark *J-V* curves for the hole-only devices. (b) Nyquist plots for the 2D and VR-2D PSCs.

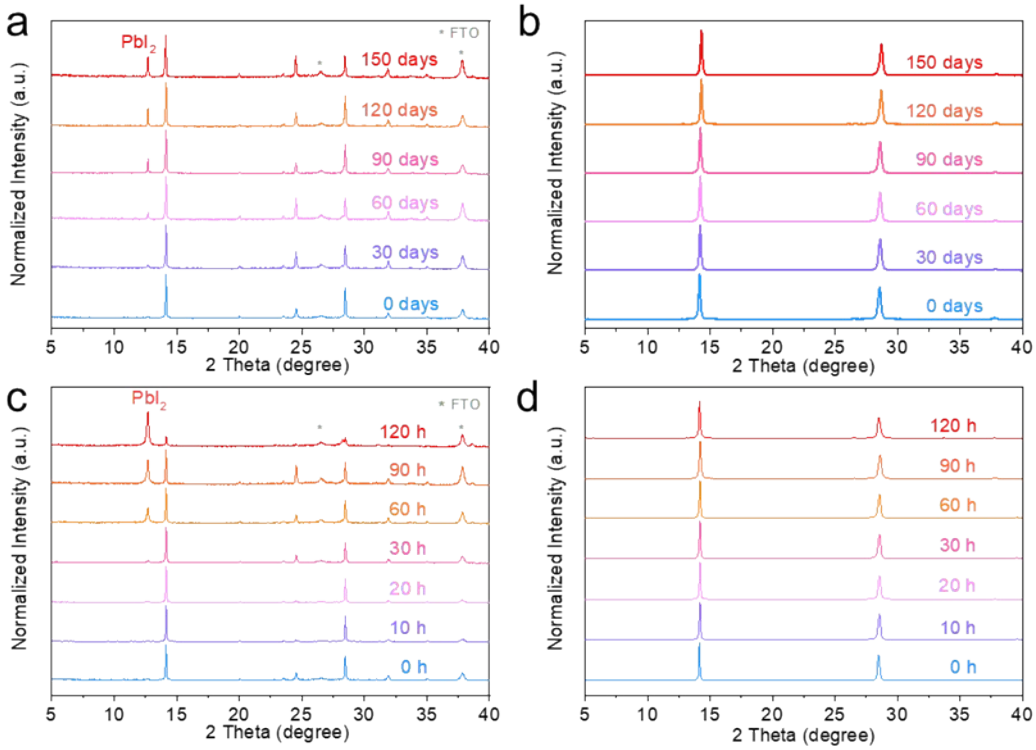

Fig. S12 (a) XRD patterns of the fresh and aging 3D $MAPbI_3$ films and (b) XRD patterns of the fresh and aging VR-2D $(PEA)_2(MA)_3Pb_4I_{13}$l films under 40% RH at 25℃ in dark. (c) XRD patterns of the fresh and aging 3D perovskite films and (d) XRD patterns of the fresh and aging VR-2D perovskite films at 85℃ in N_2.

Table S1 Summary of the average photovoltaic parameters of devices based on different additives, different NH_4Cl concentrations (PEAI: MAI: PbI_2: NH_4Cl = 2: 3: 4: x, molar ratio), differernt amounts of H_2O addition (vol %), and different ambient humidity.

	Devices	J_{SC} (mA·cm^{-2})	V_{OC} (V)	FF	PCE (%)
Different additives	w/o additive	1.07	1.01	57.52	0.69
	NH_4Br	12.53	1.08	55.32	7.45
	NH_4I	11.62	1.16	74.31	10.01
	NH_4Cl	14.61	1.16	76.42	12.96
	MACl	11.30	1.14	68.24	8.76
	PEACl	11.15	0.99	57.20	6.32
Different NH_4Cl concentrations	NH_4Cl 0.00	1.07	1.01	57.52	0.69
	NH_4Cl 0.25	12.53	1.14	74.82	10.67
	NH_4Cl 0.50	14.61	1.16	76.42	12.96
	NH_4Cl 0.75	13.44	1.17	74.24	11.66
	NH_4Cl 1.00	13.11	1.13	72.97	10.84
Differernt amounts of H_2O addition	H_2O 0.0	14.61	1.16	76.42	12.96
	H_2O 0.5	16.08	1.08	75.69	13.11
	H_2O 1.0	18.13	1.08	74.04	14.53
	H_2O 1.5	17.55	1.04	71.08	13.02
	H_2O 2.0	17.19	1.04	70.24	12.54
Different ambient humidity	10% RH	16.22	1.16	77.08	14.45
	20% RH	17.71	1.16	77.84	15.95
	30% RH	18.14	1.16	78.47	16.55
	40% RH	17.88	1.15	74.42	15.34
	50% RH	17.62	1.14	71.17	14.27

Table S2 Adsorption energies of the molecular cations at the highlighted positions of Figure 1. Adsorption energies of NH_4 and of MA (eV) and their difference (Δ, eV).

	202-surface		111-surface	
	PbI_2-ter	MAI-ter	PbI_2-ter	MAI-ter
Ads. En. of NH_4 (eV)	-8.09	-5.90	-6.54	-7.39
Ads. En. of MA (eV)	-7.94	-5.77	-6.33	-7.21
$\Delta(NH_4\text{-MA})$ (eV)	0.17	0.13	0.20	0.21

Table S3 Comparison of hole (μ_h) and electron (μ_e) mobilities and carrier lifetimes (τ_r) between VR-2D PSCs and other similar 2D PSCs.

Perovskite	Method	μ_h ($cm^2\ V^{-1}\ s^{-1}$)	μ_e ($cm^2\ V^{-1}\ s^{-1}$)	τ_r	PCE
$(PEA)_2MA_4Pb_5I_{16}$ (n = 5)	NH_4SCN additive	4.21×10^{-4}	2.64×10^{-3}	—	11.10%[6]
$(4FPEA)_2MA_4Pb_5I_{16}$ (n = 5)	NH_4SCN additive	4.09×10^{-3}	3.4×10^{-3}	—	17.34%[6]
$(PEA)_2(MA)_4Pb_5I_{16}$ (n = 5)	NH_4SCN additive	$(2.28 \pm 0.56) \times 10^{-3}$	$(2.71 \pm 1.55) \times 10^{-3}$	—	11.01%[7]
$(PEA)_2Pb_6MA_5X_{19}$ (n = 6)	MAAc + Hot casting	8.52×10^{-4}	6.44×10^{-4}	—	12.78%[8]
$(FPEA)_2MA_2Pb_3I_{10}$ (n = 6)	Direct spin coating	3.02×10^{-4}	2.84×10^{-4}	72.00 ns (TRPL)	5.80%[9]
$(PEA)_2MA_4Pb_5I_{16}$ (n = 5)	NH_4SCN + NH_4Cl	$(1.8 \pm 0.5) \times 10^{-3}$	$(6.6 \pm 1.9) \times 10^{-3}$	—	13.50%[10]
$(BDA)MA_4Pb_5X_{16}$ (n = 5)	MAAc + Hot casting	1.67 × 10−3	1.14×10^{-3}	57.80 ns (TRPL)	17.91%[11]
$(BA)_2(MA_{0.76}FA_{0.19}Cs_{0.05})_3Pb_4I_{13}$ (n = 4)	Hot casting	—	—	~100 ns (TRPL)	15.58%[12]
$(BA)_2MA_3Pb_4I_{13}$ (n = 4)	Hot casting	—	4.10×10^{-4}	68.80 μs (IMVS)	14.28%[13]
$(BA)_2MA_3Pb_4I_{13}$ (n = 4)	Hot casting	—	—	1.72 μs (IMVS)	12.51%[14]

$(BA)_2MA_3Pb_4I_{13}$ (n = 4)	Antisolvent	—	1.65×10^{-3}	27.31 μs (IMVS)	11.76%[15]
$(PEA_{0.8}BA_{0.2})_2MA_3Pb_4I_{13}$ (n = 4)	Hot casting	4.15×10^{-3}	—	1.45ms (IMVS)	15.70%[16]
$(PDMA)(MA)_9Pb_{10}I_{31}$ (n = 10)	Antisolvent	—	—	~60 ms (IMVS)	15.60%[17]
$(PEA)_2MA_3Pb_4I_{13}$ (n = 4)	**H_2O + NH_4Cl**	**7.20×10^{-3}**	**3.56×10^{-3}**	**4.24 ms (IMVS)**	**17.03% (this work)**

Table S4 Fitting parameters of TRPL results.

Samples	τ_1(ns)	% of τ_1	τ_2(ns)	% of τ_2	τ_{ave}(ns)
2D perovskite film	2.62	35.55	23.72	64.45	16.22
VR-2D perovskite film	2.24	39.54	11.66	60.46	7.94

Table S5 Comparison of power conversion efficiencies (PCEs) and stabilities between VR-2D PSCs and reported representative 2D PSCs.

Perovskite (PVK)	Method	Device structure	Degradation condition and retained PCE of the initial PCE	PCE
$(BA)_2(MA)_3Pb_4I_{13}$ (n = 4)	Hot casting	ITO/TiO_2/ PVK/Spiro-OMeTAD/Au	Dark, 40-50% RH, retained 68% of PCE after 1000 h	11.76%[15]
$(BA)_2(MA)_3Pb_4I_{13}$ (n = 4)	Hot casting	ITO/PEDOT:PSS/PVK/PCBM/Al	Dark, 65% RH, retained ~20% (unencapsulated) after 60 h and ~100% (encapsulated) for 650 h	12.52%[18]
$(BA)_2(MA)_2Pb_4I_{13}$ (n = 4)	NH_4Cl	ITO/PEDOT:PSS/PVK/PCBM/BCP/Ag	One-sun 100 mW cm^{-2}, in air, (encapsulated), retained 95% after 500 h	13.20%[19]
$(BA_{0.95}Cs_{0.05})_2(MA)_3Pb_4I_{13}$ (n = 4)	Hot-casting	FTO/TiO_2/ PVK/Spiro-OMeTAD/Au	Dark, 30% RH, retained 89% for 1400h; Dark, 80 ℃, in N_2 atmosphere, retained 85% after 16 h	13.68%[20]
$(BA)_2(MA_{0.76}FA_{0.19}Cs_{0.05})_3Pb_4I_{13}$ (n = 4)	Hot casting	ITO/MoO_3/PEDOT:PSS/PVK/PCBM/BCP/Ag	Dark, 85 ℃, keeping 80% of PCE after 1400 h	15.58%[12]

$(BEA)_2(MA)_3Pb_4I_{13}$ (n = 4)	Hot casting	ITO/PEDOT:PSS/PVK/PCBM/LiF/Al	Dark, in N_2 atmosphere, remained 83.10% after 3500 h	16.10%[21]
$(BA)_2(MA)_3Pb_4I_{13}$ (n = 4)	Slow post annealing	ITO/PTAA/PVK/C_{60}/BCP/Ag	Dark, under N_2 environment, retaining 96% after 2000 h	17.26%[22]
$(BDA)MA_4Pb_5X_{16}$ (n = 5)	MAAc + Hot casting	ITO/PEDOT:PSS/PVK/PCBM/LiF/Au	Dark, ~60% RH, retaining 84% of PCE after 1182 h	17.91%[11]
$(PEA)_2(MA)_4Pb_5I_{16}$ (n = 5)	NH_4SCN additive	ITO/PEDOT:PSS/PVK/PCBM/BCP/Ag	Dark, ~55% RH, retained 78.5% of PCE after 160 h	11.01%[7]
$(PEA)_2MA_4Pb_5I_{16}$ (n = 5)	NH_4SCN + NH_4Cl	ITO/PEDOT:PSS/PVK/PCBM/BCP/Ag	Dark, 30% RH, retained 90% of PCE after 45 days	14.10%[23]
$(FPEA)_2(MA)_4Pb_5I_{16}$ (n = 5)	NH_4SCN + NH_4Cl	ITO/PEDOT:PSS/PVK/PCBM/BCP/Ag	Dark, 40-50% RH, keeping 90% of the PCE after 40 d	14.50%[10]
$(ThMA)_2(MA)_2Pb_3I_{10}$ (n = 3)	MACl	ITO/PEDOT:PSS/PVK/PCBM/BCP/Ag	Dark, under N_2 environment, retaining 90% of PCE after 1000 h	15.42%[24]
$(PEA_{0.8}BA_{0.2})_2MA_3Pb_4I_{13}$ (n = 4)	Hot casting	ITO/PTAA/PVK/PCBM/BCP/Ag	Dark, 40%-50% RH, keeping 88% of the initial PCE after 720 h	15.70%[16]
$(4FPEA)_2MA_4Pb_5I_{16}$ (n = 5)	NH_4SCN additive	ITO/PTAA/PVK/PCBM/PEI/Ag	Dark 55-65% RH, keeping 93% for 500h; 55 ℃, in N_2 atmosphere, keeping over 90% after 500 h	17.34%[6]
$(MTEA)_2(MA)_4Pb_5I_{16}$ (n = 5)	Hot casting	ITO/PEDOT:PSS/PVK/PCBM/Cr/Au	Continuous power output at the MPP, keeping 87.1% for 1000 h	18.06%[25]
$(BBAI)_2MA_{n-1}Pb_nI_{3n+1}$ (3<n<4)	Hot casting	ITO/PTAA/PVK/PCBM/Cr/Ag	Dark, ~40% RH, keeping 82% of its initial PCE after 2400 h.	18.20%[26]
$(PEA)_2MA_3Pb_4I_{13}$ (n = 4)	**H_2O + NH_4Cl**	**ITO/PEDOT:PSS/PVK/PCBM/BCP/Ag**	**Dark, ~40% RH, retained 90% of the initial PCE after 3600 h; Dark, 85 ℃, in N_2 atmosphere, retained over**	**17.03% (this work)**

90% after 1600 h

References

1. P. Giannozzi, S. Baroni, N. Bonini, M. Calandra, R. Car, C. Cavazzoni, D. Ceresoli, G. L. Chiarotti, M. Cococcioni, I. Dabo, A. D. Corso, S. de Gironcoli, S. Fabris, G. Frates, R. Gebauer, U. Gerstmann, C. Gougoussis, A. Kokalj, M. Lazzeri, L. Martin-Samos, N. Marzari, F. Mauri, R. Mazzarello, S. Paolini, A. Pasquarello, L. Paulatto, C. Sbraccia, S. Scandolo, G. Sclauzero, A. P. Seitsonen, A. Smogunov, P. Umari, R. M. Wentzcovitch, QUANTUM ESPRESSO: A Modular and Open-Source Software Project for Quantum Simulations of Materials. J. *Phys.: Condens. Matter* 2009, **21**, 395502.

2. S. Grimme, J. Antony, S. Ehrlich, H. Krieg, A consistent and accurate ab initio parametrization of density functional dispersion correction (DFT-D) for the 94 elements H-Pu. *J. Chem. Phys*. 2010, **132**, 154104.

3. Perdew, J. P.; Burke, K.; Ernzerhof, M., Generalized Gradient Approximation Made Simple. Phys. Rev. Lett. 1996, 77, 3865-3868.

4. D. Vanderbilt, Soft self-consistent pseudopotentials in a generalized eigenvalue formalism. *Phys. Rev. B* 1990, **41**, 7892-7895.

5. Y. Yang, H. Peng, C. Liu, Z. Arain, Y. Ding, S. Ma, X. Liu, T. Hayat, A. Alsaedi and S. Dai, *J. Mater. Chem. A*, 2019, **7**, 6450-6458.

6. J. Shi, Y. Gao, X. Gao, Y. Zhang, J. Zhang, X. Jing and M. Shao, *Adv. Mater.*, 2019, **31**, 1901673.

7. X. Zhang, G. Wu, W. Fu, M. Qin, W. Yang, J. Yan, Z. Zhang, X. Lu and H. Chen, *Adv. Energy Mater.*, 2018, **8**, 1702498.

8. H. Chen, Y. Xia, B. Wu, F. Liu, T. Niu, L. Chao, G. Xing, T. Sum, Y. Chen and W. Huang, *Nano energy*, 2019, **56**, 373-381.

9. H. Pan, X. Zhao, X. Gong, Y. Shen and M. Wang, *J. Phys. Chem. Lett.*, 2019, **10**, 1813-1819.

10. W. Fu, H. Liu, X. Shi, L. Zuo, X. Li and A. K. Y. Jen, A*dv. Funct. Mater.*, 2019,

29, 1900221.

11. T. Niu, H. Ren, B. Wu, Y. Xia, X. Xie, Y. Yang, X. Gao, Y. Chen and W. Huang, *J. Phys. Chem. Lett.*, 2019, **10**, 2349-2356.

12. Y. Jiang, X. He, T. Liu, N. Zhao, M. Qin, J. Liu, F. Jiang, F. Qin, L. Sun and X. Lu, *ACS Energy Lett.*, 2019, **4**, 1216-1224.

13. G. Wu, J. Zhou, J. Zhang, R. Meng, B. Wang, B. Xue, X. Leng, D. Zhang, X. Zhang and S. Bi, *Nano Energy*, 2019, **58**, 706-714.

14. S. Tan, N. Zhou, Y. Chen, L. Li, G. Liu, P. Liu, C. Zhu, J. Lu, W. Sun and Q. Chen, *Adv. Energy Mater.*, 2019, **9**, 1803024.

15. T. He, S. Li, Y. Jiang, C. Qin, M. Cui, L. Qiao, H. Xu, J. Yang, R. Long and H. Wang, *Nat. Commun.*, 2020, **11**, 1-11.

16. S. Chen, N. Shen, L. Zhang, W. Kong, L. Zhang, C. Cheng and B. Xu, *J. Mater. Chem. A*, 2019, **7**, 9542-9549.

17. B.-E. Cohen, Y. Li, Q. Meng and L. Etgar, *Nano Lett.*, 2019, **19**, 2588-2597.

18. H. Tsai, W. Nie, J.-C. Blancon, C. C. Stoumpos, R. Asadpour, B. Harutyunyan, A. J. Neukirch, R. Verduzco, J. J. Crochet and S. Tretiak, *Nature*, 2016, **536**, 312.

19. J. Wang, S. Luo, Y. Lin, Y. Chen, Y. Deng, Z. Li, K. Meng, G. Chen, T. Huang, S. Xiao, H. Huang, C. Zhou, L. Ding, J. He, J. Huang and Y. Yuan, *Nat. Commun.*, 2020, **11**, 582.

20. X. Zhang, X. Ren, B. Liu, R. Munir, X. Zhu, D. Yang, J. Li, Y. Liu, D.-M. Smilgies and R. Li, *Energy Environ. Sci.*, 2017, **10**, 2095-2102.

21. L. Chao, T. Niu, Y. Xia, X. Ran, Y. Chen and W. Huang, *J. Phys. Chem. Lett.*, 2019, **10**, 1173-1179.

22. G. Wu, X. Li, J. Zhou, J. Zhang, X. Zhang, X. Leng, P. Wang, M. Chen, D. Zhang and K. Zhao, *Adv. Mater.*, 2019, **31**, 1903889.

23. W. Fu, J. Wang, L. Zuo, K. Gao, F. Liu, D. S. Ginger and A. K.-Y. Jen, *ACS Energy Lett.*, 2018, **3**, 2086-2093.

24. H. Lai, B. Kan, T. Liu, N. Zheng, Z. Xie, T. Zhou, X. Wan, X. Zhang, Y. Liu and Y. Chen, *J. Am. Chem. Soc.*, 2018, **140**, 11639-11646.

25. H. Ren, S. Yu, L. Chao, Y. Xia, Y. Sun, S. Zuo, F. Li, T. Niu, Y. Yang and H. Ju,

Nat. Photonics, 2020, **14**, 1-10.

26. R. Yang, R. Li, Y. Cao, Y. Wei, Y. Miao, W. L. Tan, X. Jiao, H. Chen, L. Zhang, Q. Chen, H. Zhang, W. Zou, Y. Wang, M. Yang, C. Yi, N. Wang, F. Gao, C. R. McNeill, T. Qin, J. Wang and W. Huang, *Adv. Mater.*, 2018, **30**, 1804771.